

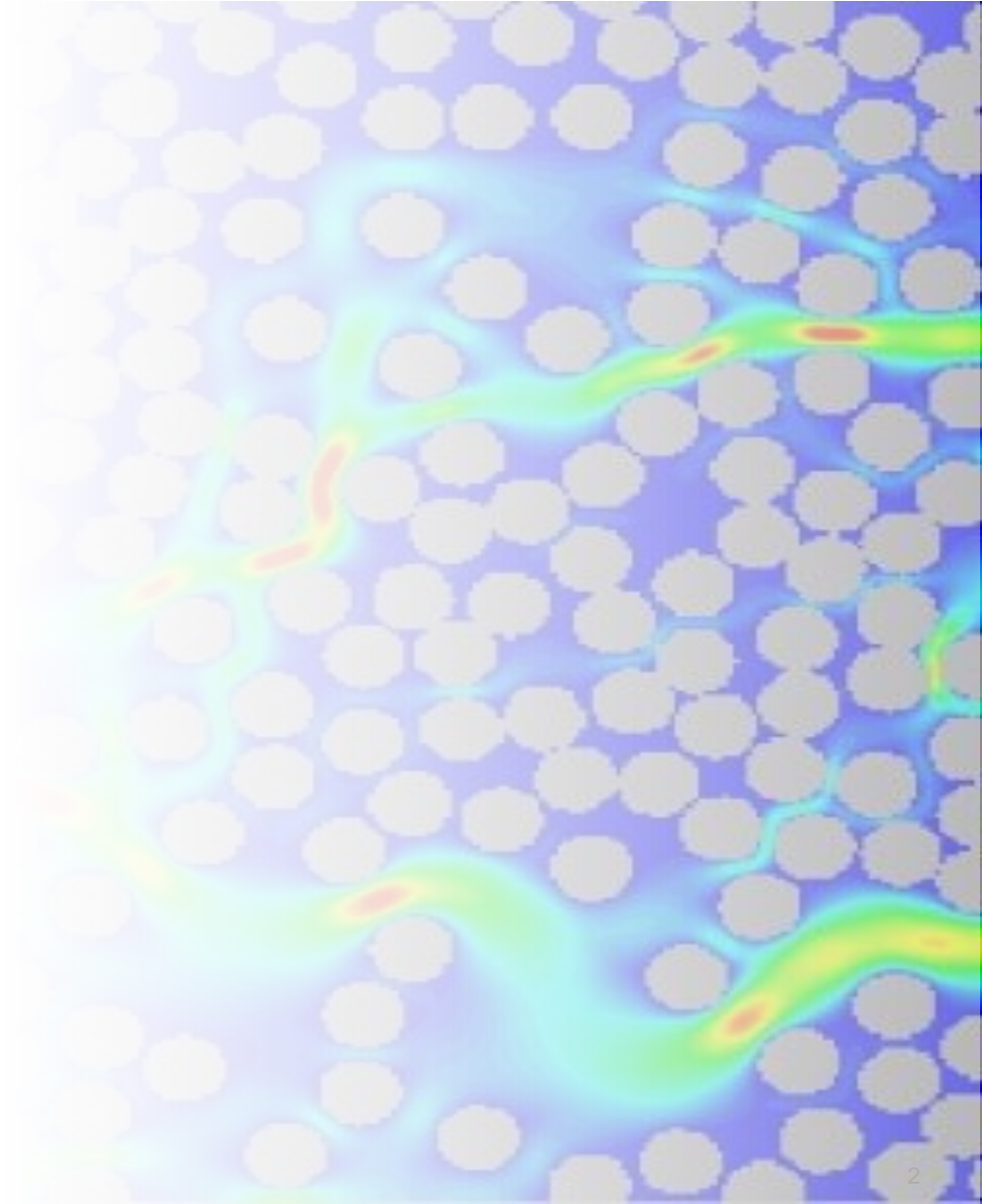
Micro-Scale Results from the Benchmark Exercise on the Image-Based Permeability Prediction of Composite Reinforcements

Elena Syerko, Christophe Binetruy, Tim Schmidt, David May

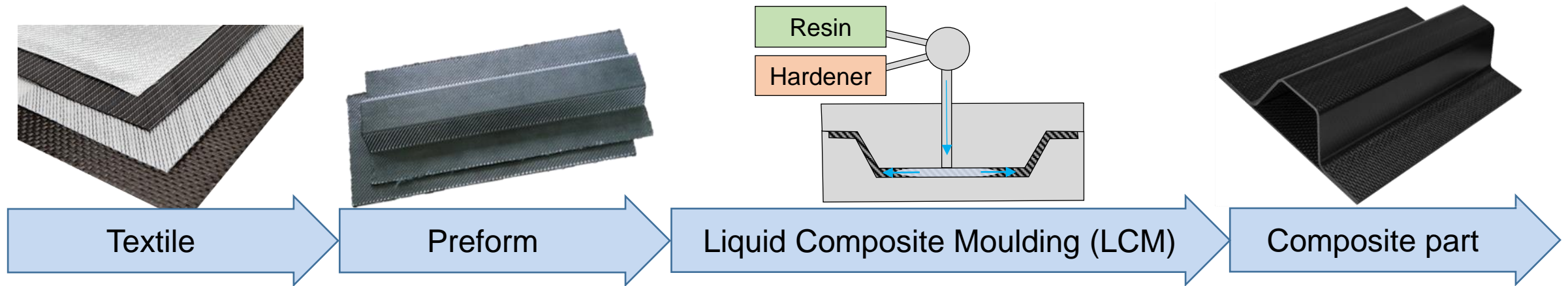
Image-Based Simulation for Industry - 2022

London, 17-21 October 2022

1. Context
2. Motivation and objectives of the benchmark
3. Benchmark approach
4. Input image data for micro-scale stage
5. Analysis of micro-scale results
6. Conclusions and way forward



Liquid Composite Moulding (LCM) Process



Darcy's law:

volume-averaged flow velocity

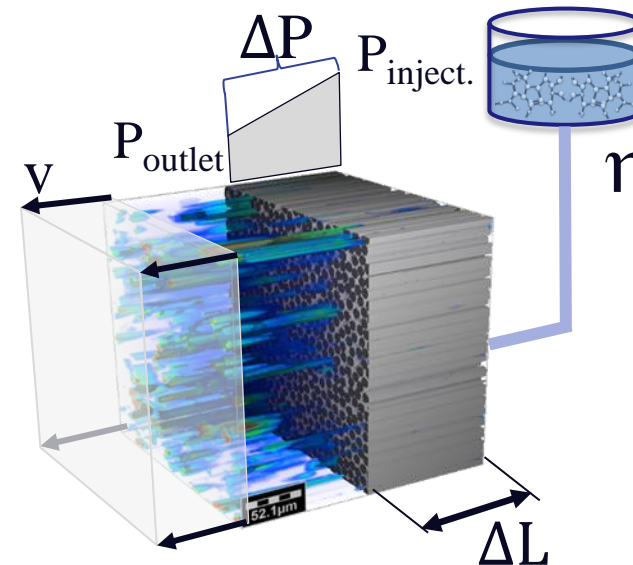
$$v = - \frac{K}{\eta} \cdot \frac{\Delta P}{\Delta L}$$

viscosity

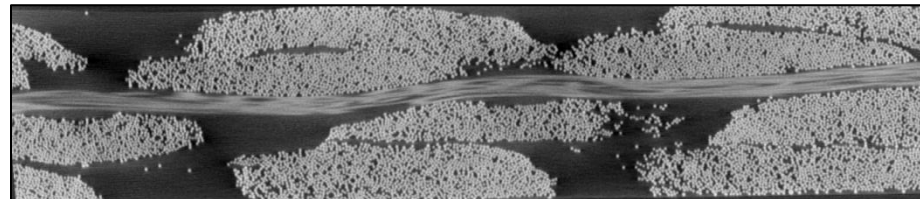
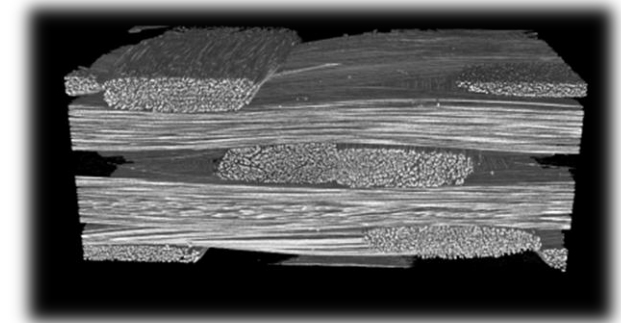
Permeability

pressure drop

flow length

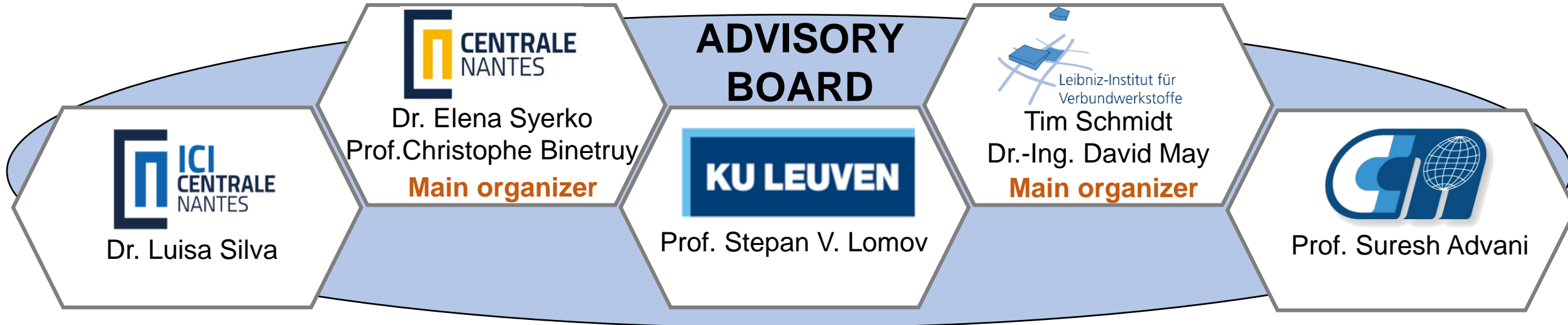


1. Fiber reinforcements in composites are special class of porous media:
 - *dual-scale porosity*,
 - *anisotropy*,
 - *variability*.
2. Very few commercial software to compute permeability of porous media. The majority – not designed to address multi-scale fibrous media.
3. Benchmarks of experimental measurements of permeability of fibrous preforms revealed high discrepancy of results – at least ~20% [N.Vernet et al, 2014], [D.May et al, 2019], [A.Yong et al, 2021].
4. Influence of material geometrical variability on permeability is difficult (impossible at micro-scale) to appreciate through a purely experimental effort.



Virtual Permeability Benchmark – first contribution to a real fibrous structure.

Benchmark approach



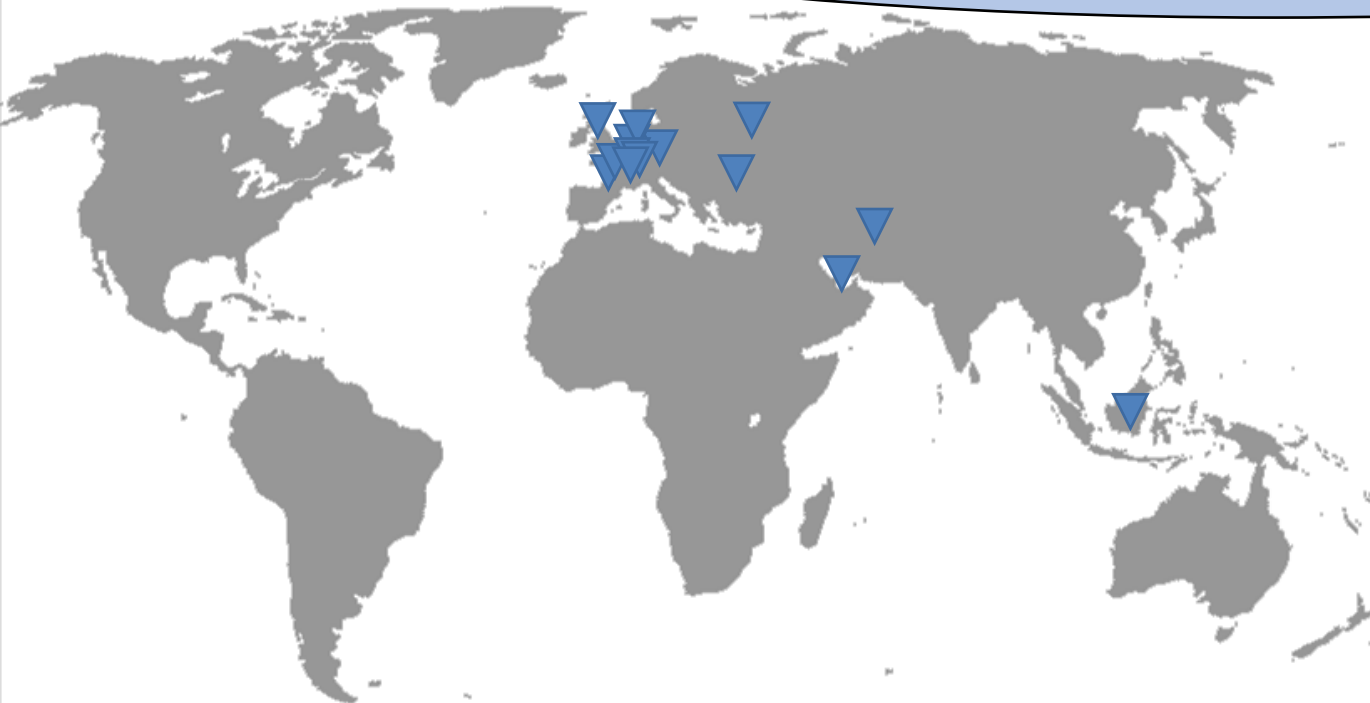
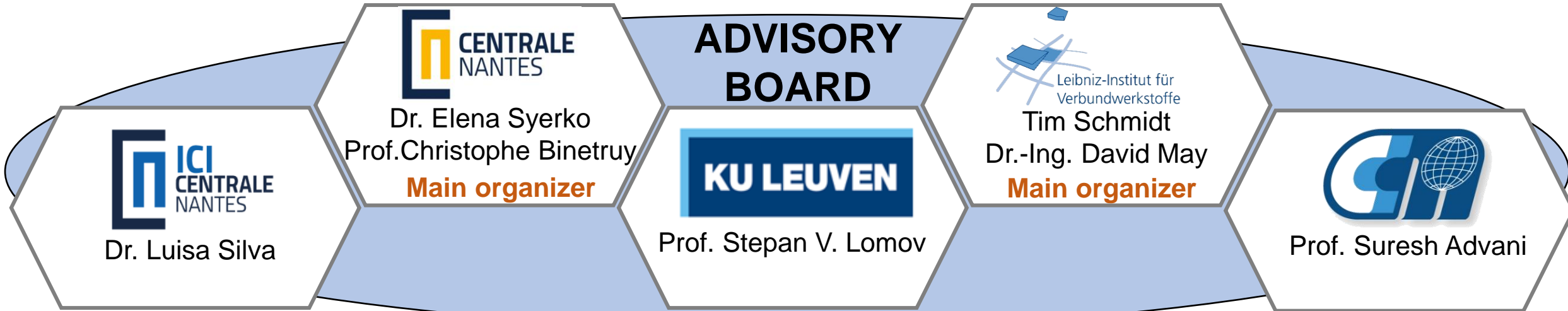
Objective: develop general guidelines for the image-based numerical prediction of permeability of engineering textiles.

- Already **segmented** images of the material are provided to eliminate possible sources of variation.
- No fixed conditions (method, boundary conditions,...) for the calculations for the first stage of the benchmark.

Choice limited by the computational resources:

- discretization;
- 2D/3D formulation;
- subdivision into sub-volumes

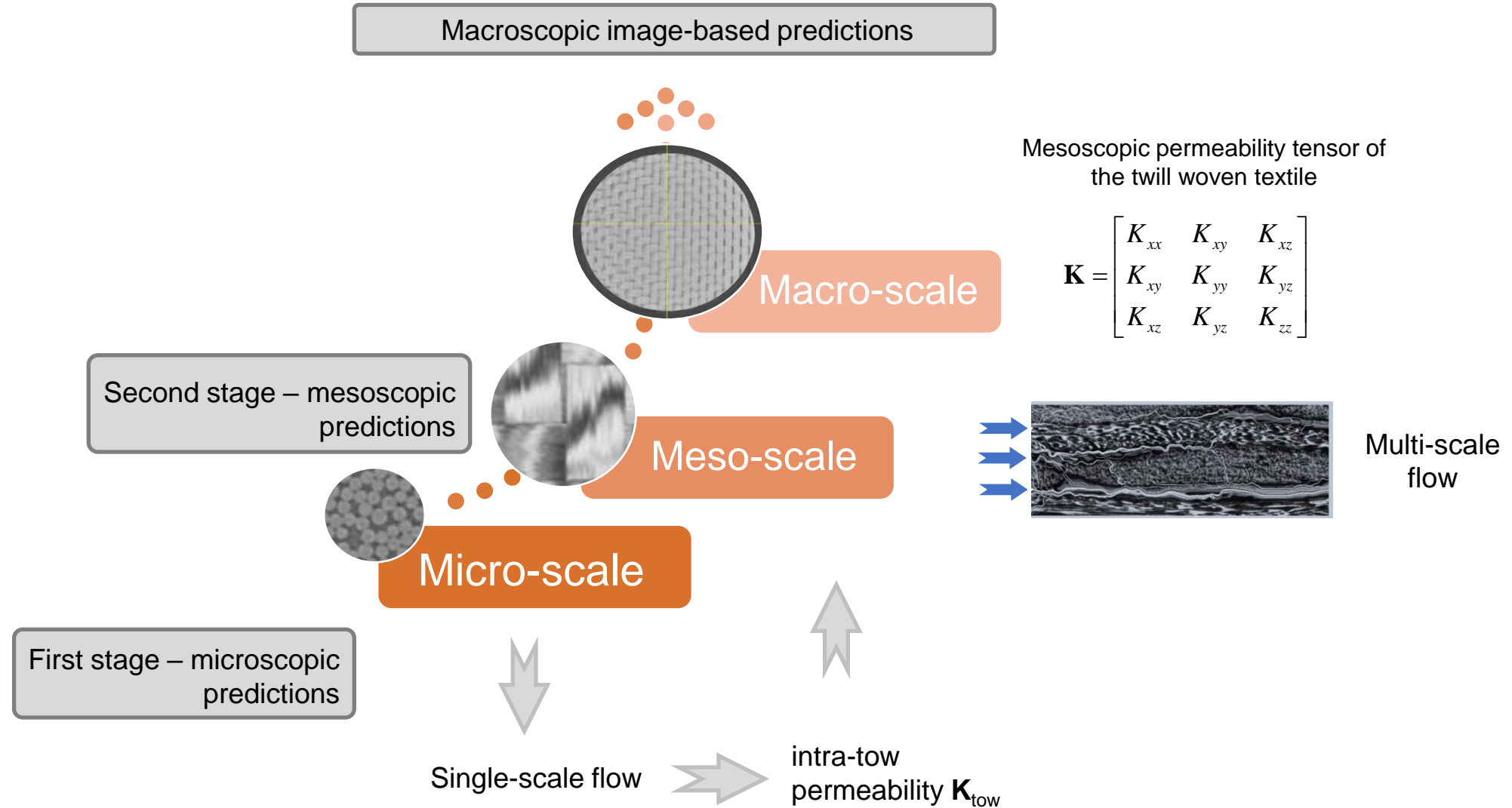
Benchmark approach



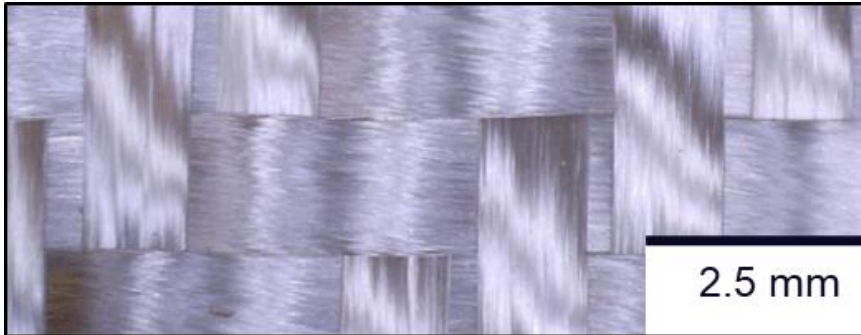
16 participants from 10 countries

- LPAC, Lausanne
- IVW, Kaiserslautern
- 3SR Lab, Grenoble
- ITWM, Kaiserslautern
- ICI, Centrale Nantes
- TENSYL, Périgny
- GeM, Centrale Nantes
- KU Leuven
- Universität Stuttgart
- University of Nottingham
- IMT Lille Douai
- RISE, Göteborg
- Ferdowski University of Mashdad
- National University of Singapore
- Skoltech, Moscow
- Mines Saint-Etienne
- Siemens Industry Software, Leuven
- Khalifa University, Abu Dhabi

Benchmark approach

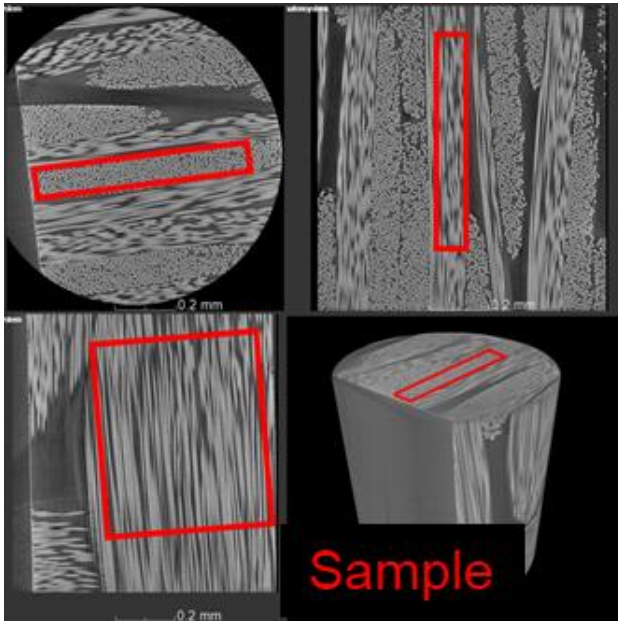


Glass fibre woven fabric (295 g/m²)



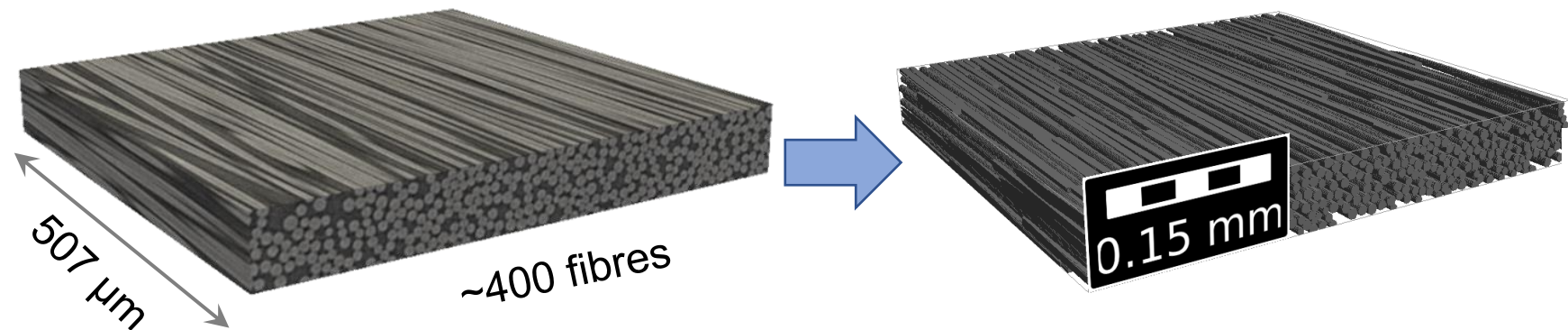
Tow specifications:

- 3 yarns twisted in a tow
- 40 twist/meter => 1 twist / 25 mm
- fibre diameter: 7.5-9.3 μm (data sheet: 9 μm)



Scan nominal resolution 0.52 μm^3

Provided segmented volume with defined two phases (~1000 x 120 x 1000 voxels)

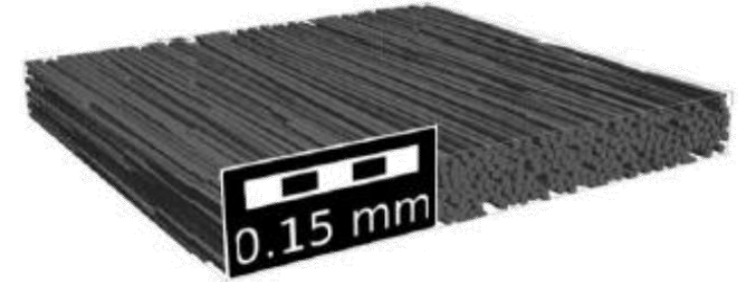
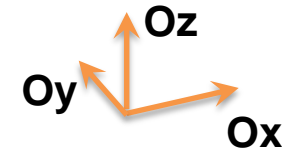
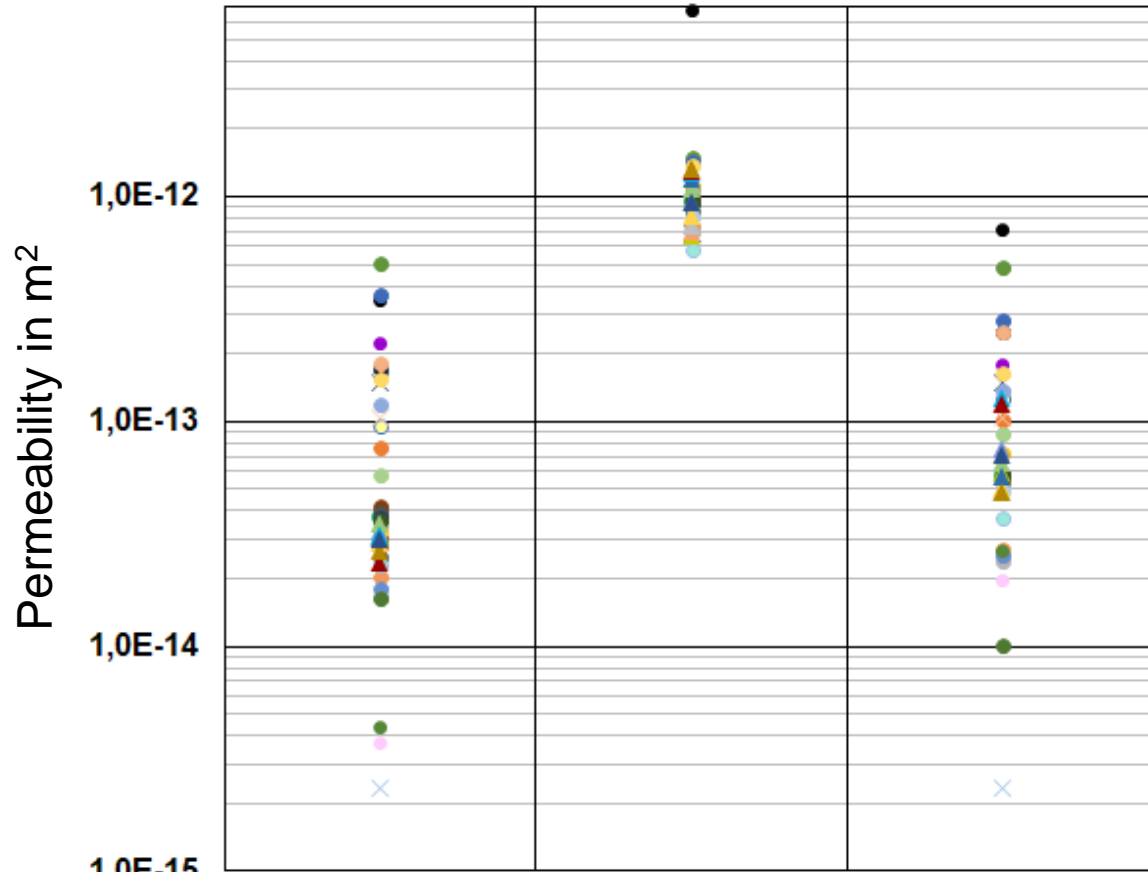


✓ Averaged over tow sample fibre volume content (FVC): 56.46%

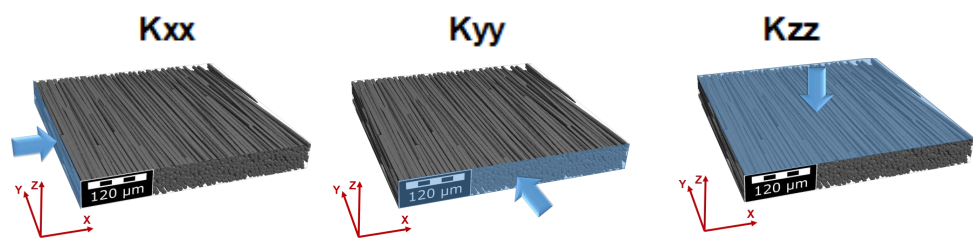
Overview of micro-scale results

16 participants delivered 50 results in total

- 1 ◦ 2a • 2b • 3 • 4a × 4b × 4c • 5 • 6a • 6b
- 6c • 7a × 7b • 8a • 8b • 9 • 10a • 10b • 11 • 12a
- 12b • 12c • 12d • 13 • 14a • 14b • 15a • 15b • 16a • 16b
- 16c • 16d • 16e • 16f • 16g • 16h • 16i • 16j • 16k • 16l
- 16m • 16n • 16o • 16p • 16q • 16r • 16s • 16t • 16u • 16v



	K_{xx}, m^2	K_{yy}, m^2	K_{zz}, m^2
Mean	7.42E-14	1.11E-12	1.05E-13
STD	1.02E-13	8.97E-13	1.25E-13
CV	137%	81%	119%

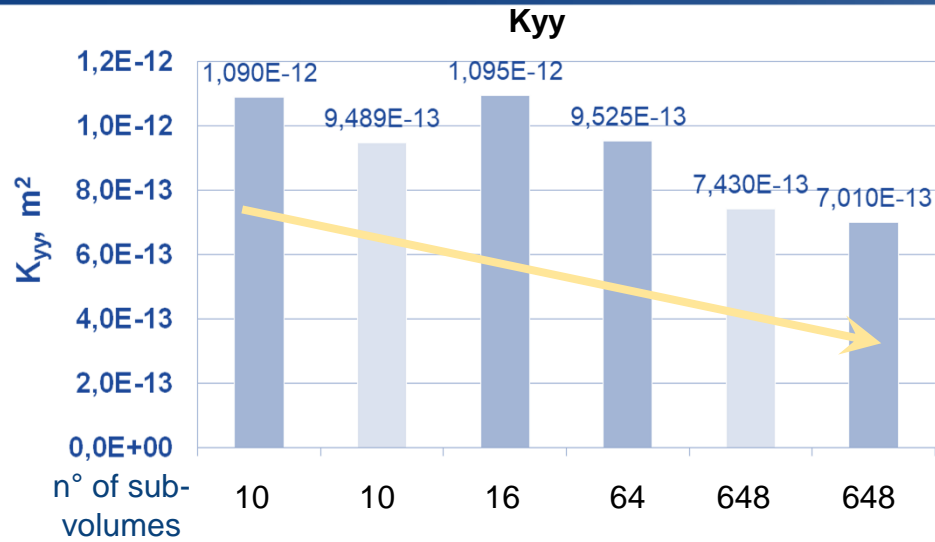


- 3 participants provided results in **2D** (without axial permeability K_{yy})
- Only two participants used the same method and settings

Overview of methods, models, and parameters used

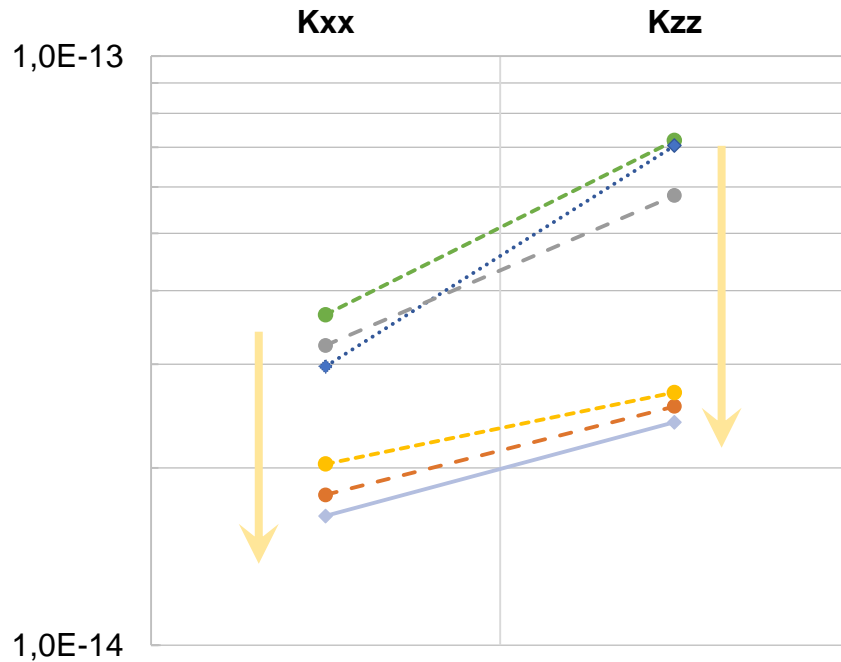
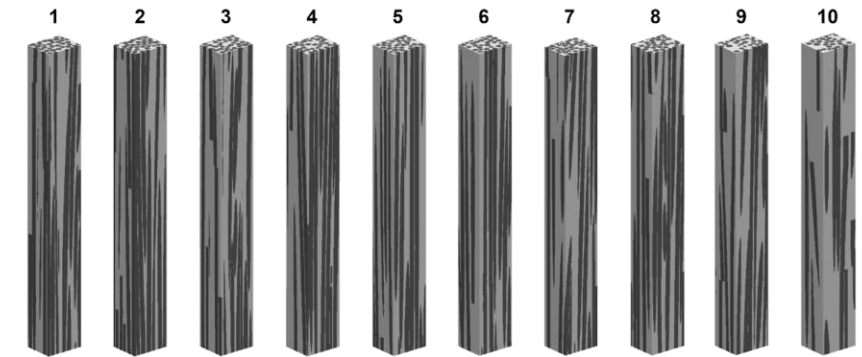
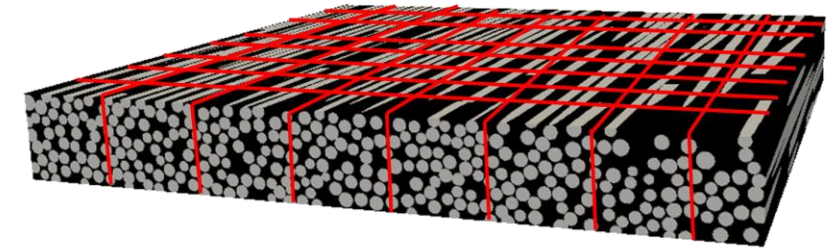
Participant #	Numerical approximation	Discretization	Flow model	2D / 3D formulation	Physical variables formulation	Model size, voxels / Voxel size, μm^3	FVC, %
1	FVM	Voxel-based	Stokes	3D	SIMPLE	1003x973x124 / $0.521^3 \mu\text{m}^3$	56.46
2	FEM	Geometry-based	Navier-Stokes	2D	mixed velocity-pressure	10 2D slices of $\approx 1003 \times 124 / 0.521^3 \mu\text{m}^3$	56.73 (55.06 – 59.54), 58.54 (57.08 – 61.39)
3	FVM	Voxel-based	Navier-Stokes	3D	mixed velocity-pressure	1800x180x200 / $0.2605 \mu\text{m} \times 2.605 \mu\text{m} \times 0.2605 \mu\text{m}$	57.00
4	CVFEM	Voxel-based	Navier-Stokes	3D	mixed velocity-pressure	10 sub-volumes of $\approx 1003 \times 100 \times 124$ for K_{xx}, K_{zz} 10 sub-volumes $\approx 100 \times 973 \times 124$ for $K_{yy} / 0.521^3 \mu\text{m}^3$	56.46 (54.02 – 58.78), 56.46 (48.42 – 60.88)
5	FVM	Voxel-based / LIR	Stokes	3D	mixed velocity-pressure	1003x973x124 / $0.521^3 \mu\text{m}^3$	56.46
6	FEM	Geometry-based	Stokes	2D	mixed velocity-pressure	973 2D slices of $1003 \times 124 / 0.521^3 \mu\text{m}^3$	55.87
7	FVM	Geometry-based	Navier-Stokes	3D	SIMPLE	1003x973x124 / $0.521^3 \mu\text{m}^3$	59.87
8	FDM	Voxel-based	Stokes	3D	mixed velocity-pressure	972x972x108: 648 sub-volumes of $54 \times 54 \times 54 / 0.521^3 \mu\text{m}^3$	57.16
9	FVM	Geometry-based	Stokes	3D	mixed velocity-pressure	16 sub-volumes of $\approx 251 \times 243 \times 124 / 0.521^3 \mu\text{m}^3$	56.36 (46.96 – 60.84)
10	FEM	Voxel-based	Stokes	3D	pseudo-compressibility (penalization)	64 sub-volumes of $\approx 126 \times 122 \times 124 / 0.521^3 \mu\text{m}^3$	56.46 (46.49 – 61.81)
11	FVM	Geometry-based	Navier-Stokes	3D	mixed velocity-pressure	1003x679x124 / $\approx 0.7368^3 \mu\text{m}^3$	58.69
12	FVM	Voxel-based / LIR	Stokes	3D	SIMPLE mixed velocity-pressure	1003x973x124 / $0.521^3 \mu\text{m}^3$	56.46
13	FVM	Geometry-based	Navier-Stokes	3D	mixed velocity-pressure	124x192x124 / $0.521^3 \mu\text{m}^3$	59.54
14	FEM	Geometry-based	Stokes	2D	mixed velocity-pressure	973 2D slices of $1003 \times 124 / 0.521^3 \mu\text{m}^3$	56.46, 55.57
15	FEM	Geometry-based	Stokes	3D	mixed velocity-pressure	1003x973x124 / $0.521^3 \mu\text{m}^3$	56.46, 51.00
16	FVM FDM	Voxel-based / LIR	Stokes	3D	SIMPLE mixed velocity-pressure	1003x973x124 / $0.521^3 \mu\text{m}^3$ 10 sub-volumes $\approx 1003 \times 100 \times 124 / 0.521^3 \mu\text{m}^3$	56.46, 56.46 (54.02 – 58.78)

Influence of cropping into sub-domains

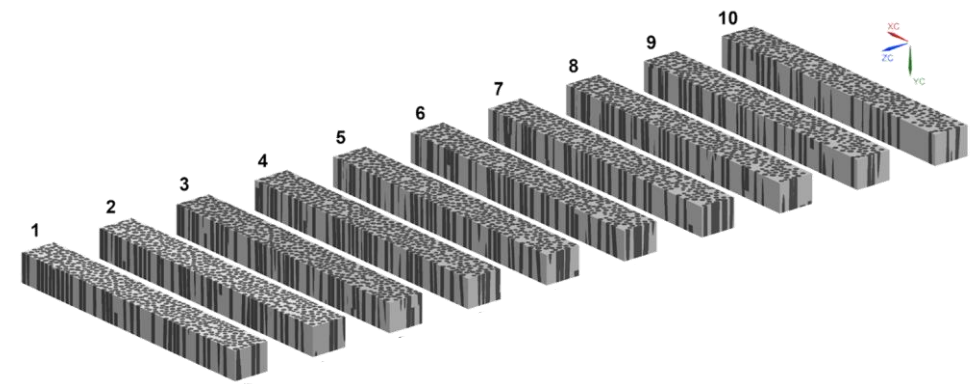


➤ **15% deviation from the main cluster mean value using 10 sub-volumes**

Arithmetic and harmonic means of values from sub-volumes

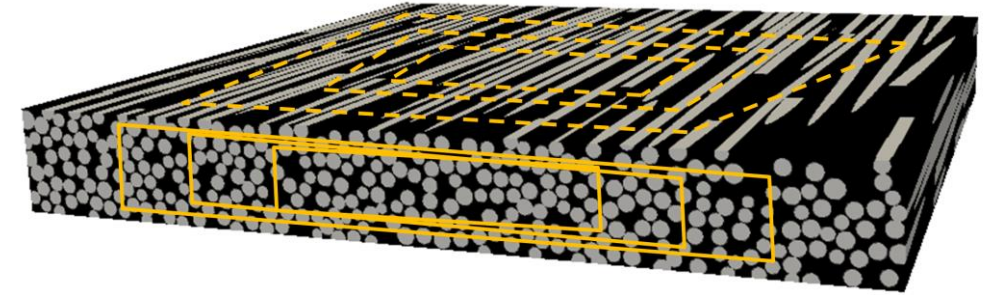
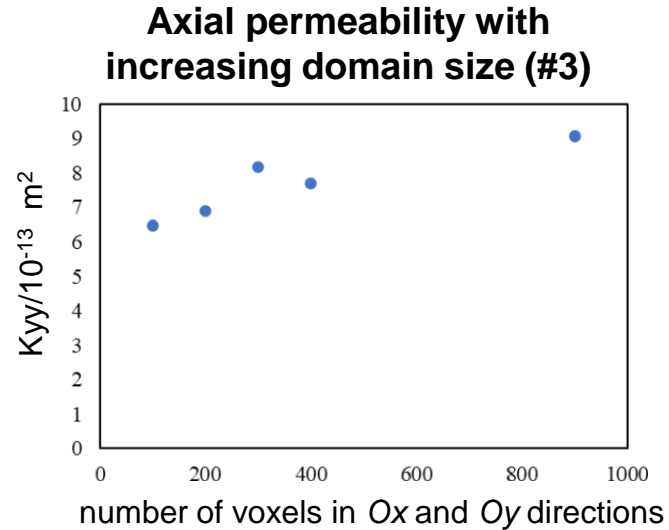


- #4a, 10 sub-volumes
- ◆--- #16v, 10 sub-volumes
- #9, 16 sub-volumes
- #10a, 64 sub-volumes
- ◆--- #8b, 648 sub-volumes
- #8a, 648 sub-volumes, Darcy

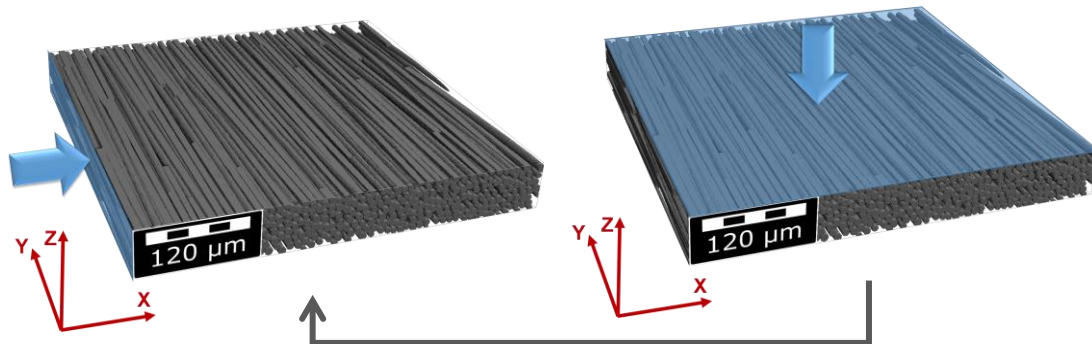


Influence of domain dimensions

- No convergence of permeability with increasing domain size up to the entire sample volume:

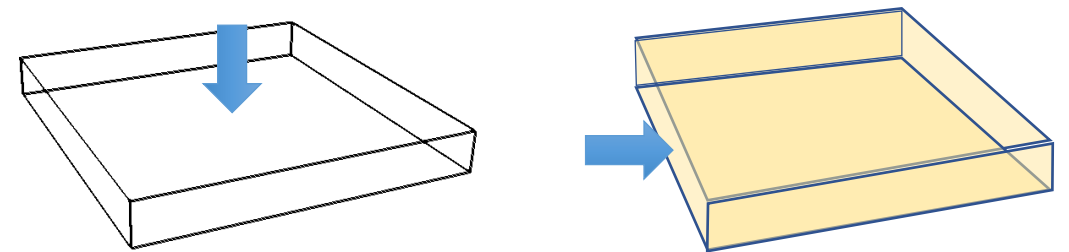


- Transverse K_{zz} is higher than transverse K_{xx}



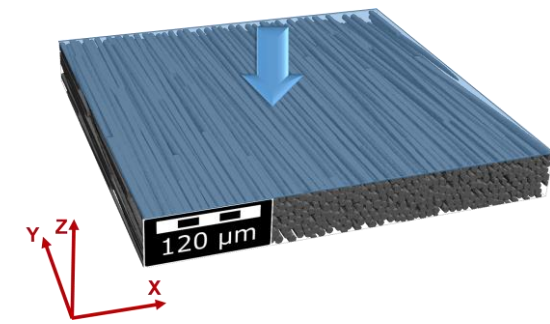
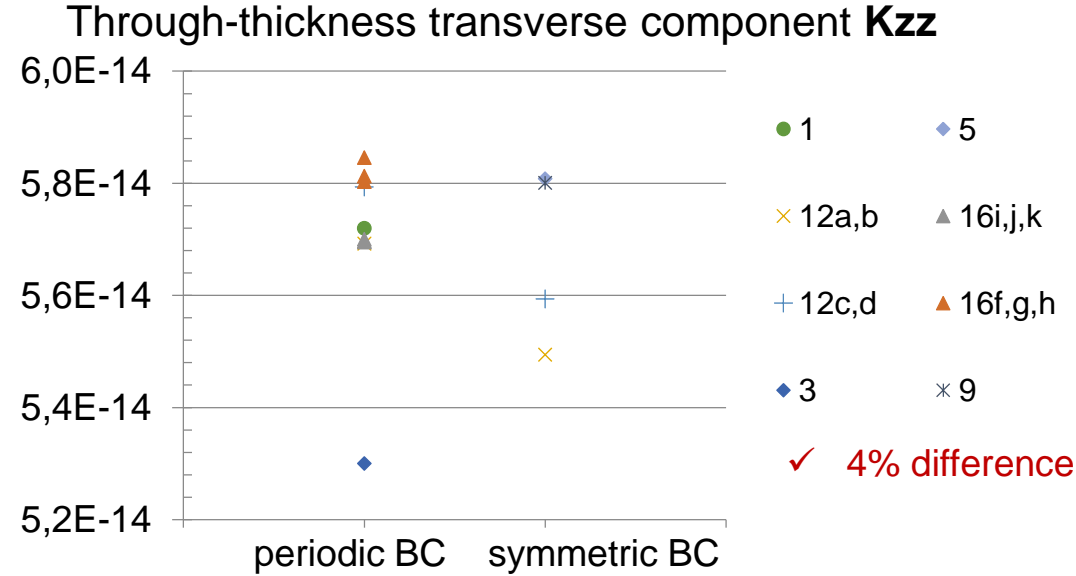
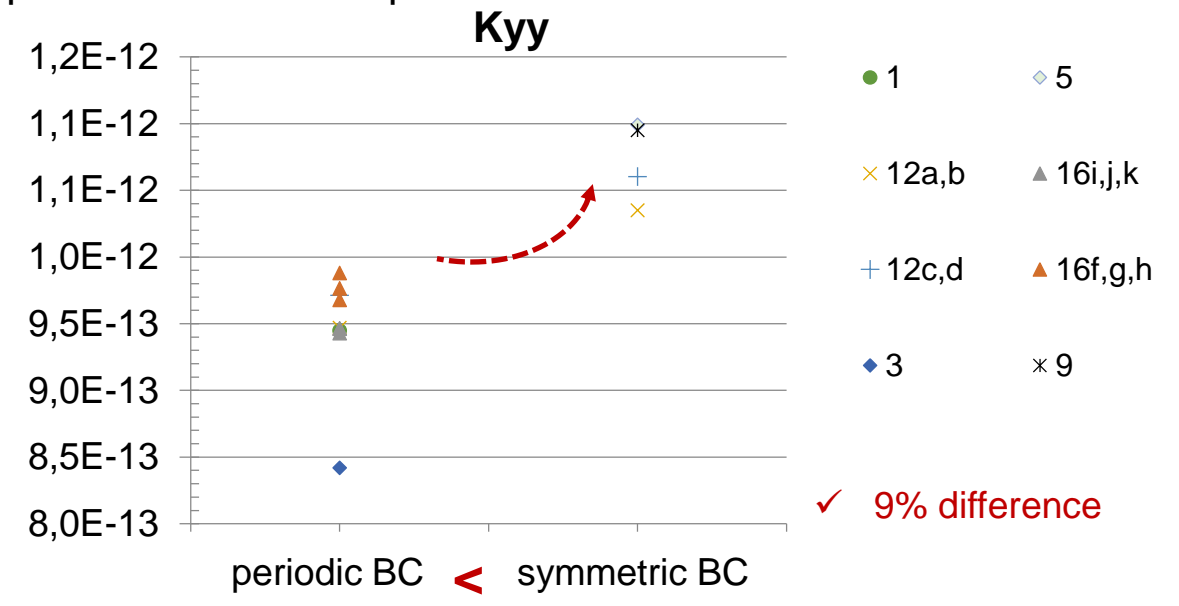
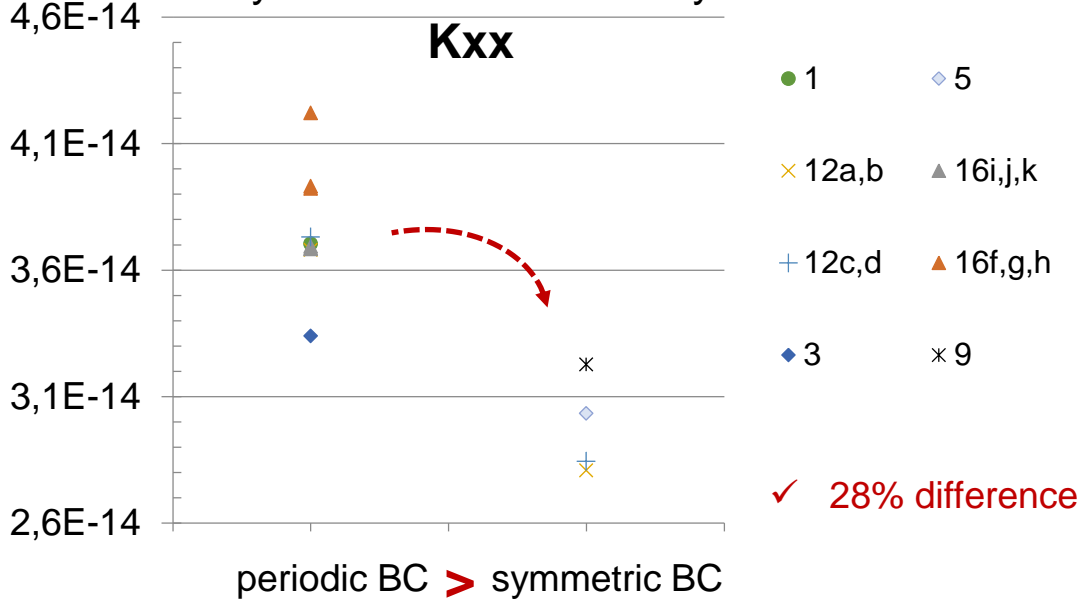
1/8th of in-plane dimensions,
not statistically representative

- Effect of BC in tangential direction for K_{zz} is minimized



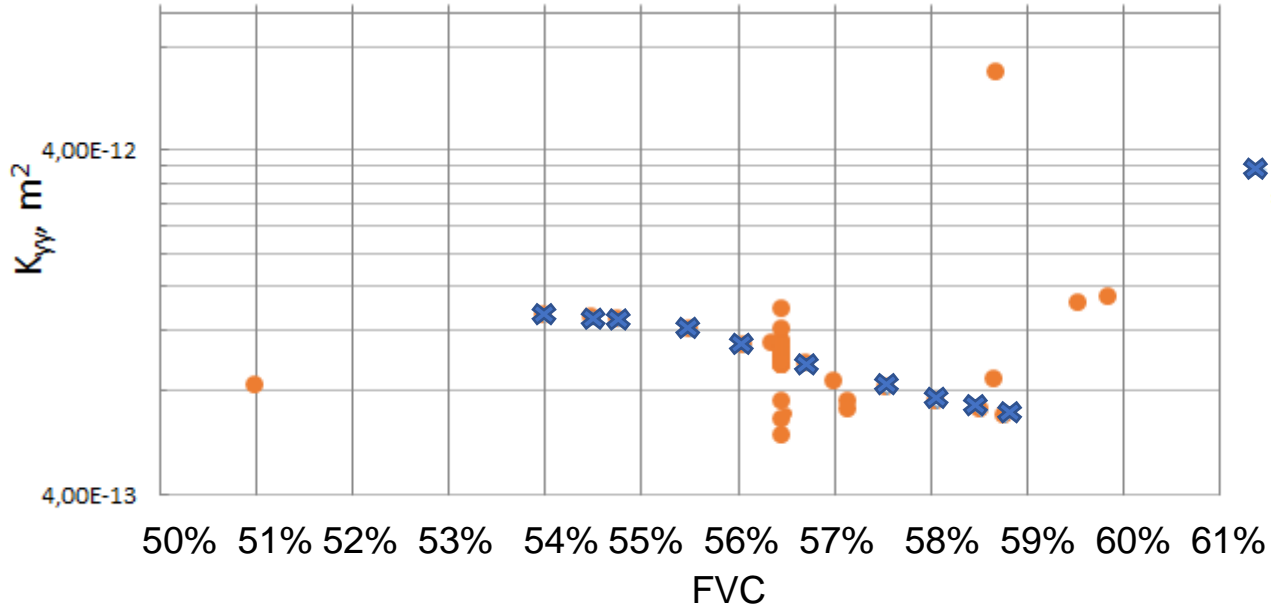
Influence of boundary conditions

➤ When only the results obtained by the same methods and parameters are compared:

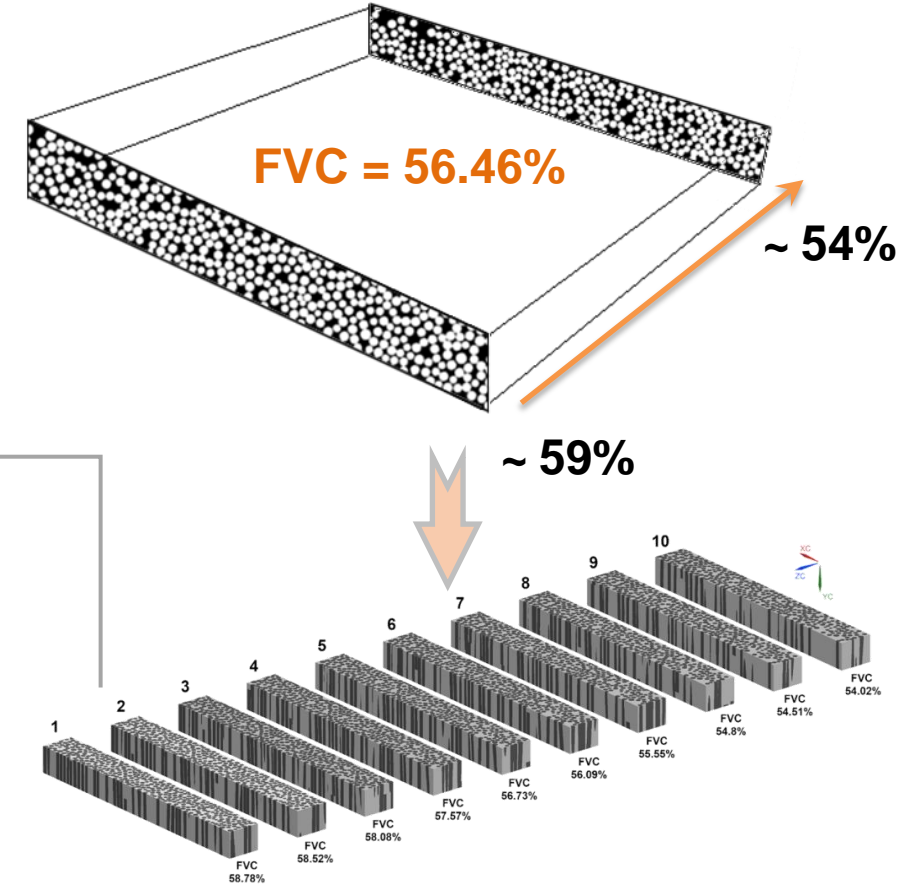


Correlation with fiber volume content

Axial permeability K_{yy}



Sub-volumes #16l-u

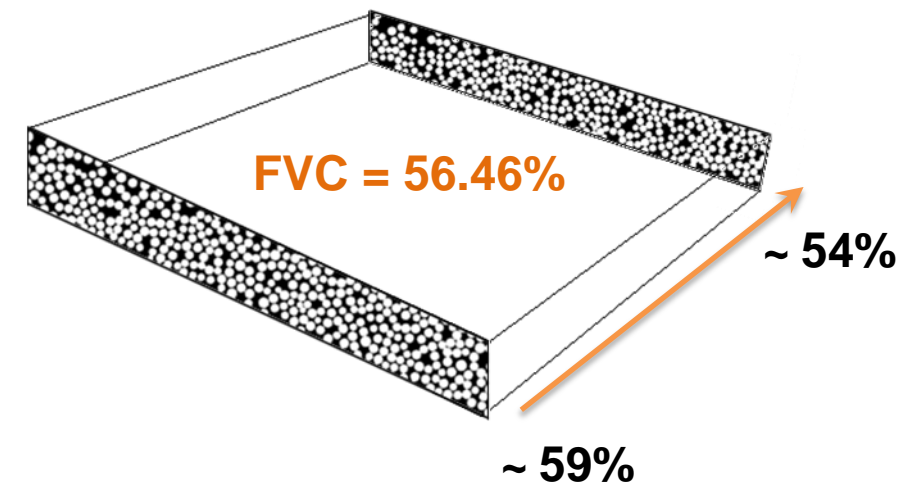
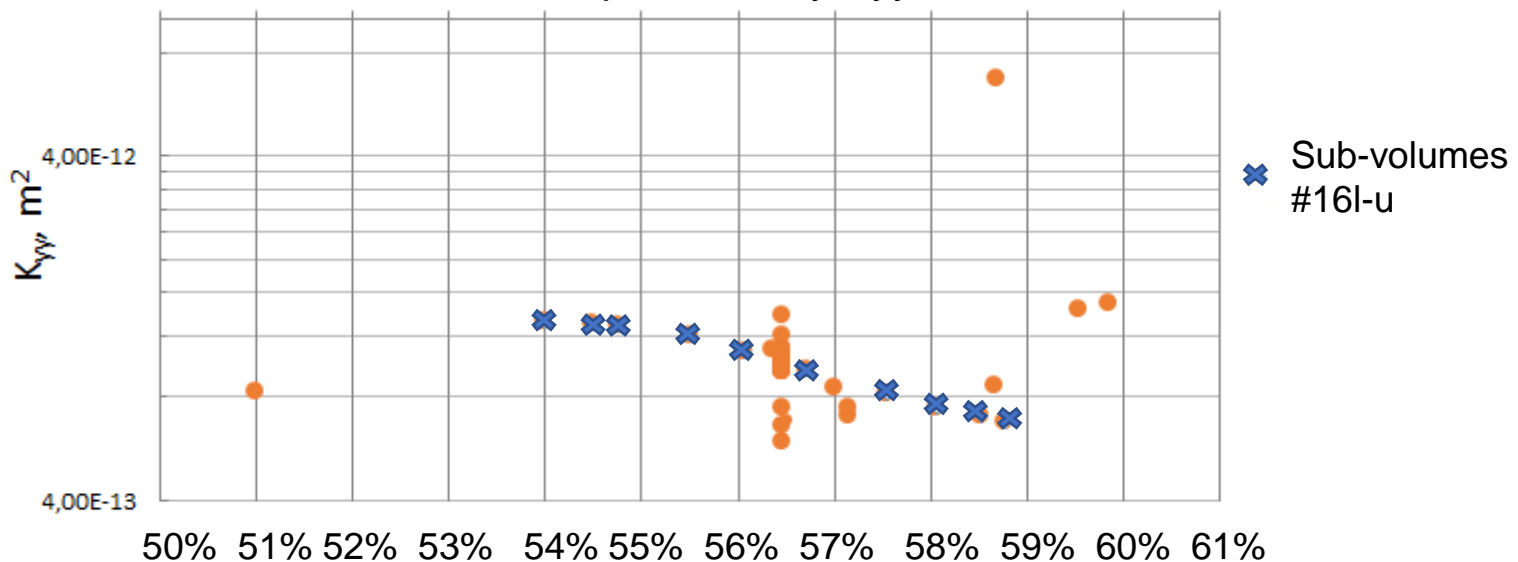


- ✓ Different FVC can result from:
 - different model sizes,
 - cropping of edges,
 - discretization of domain.

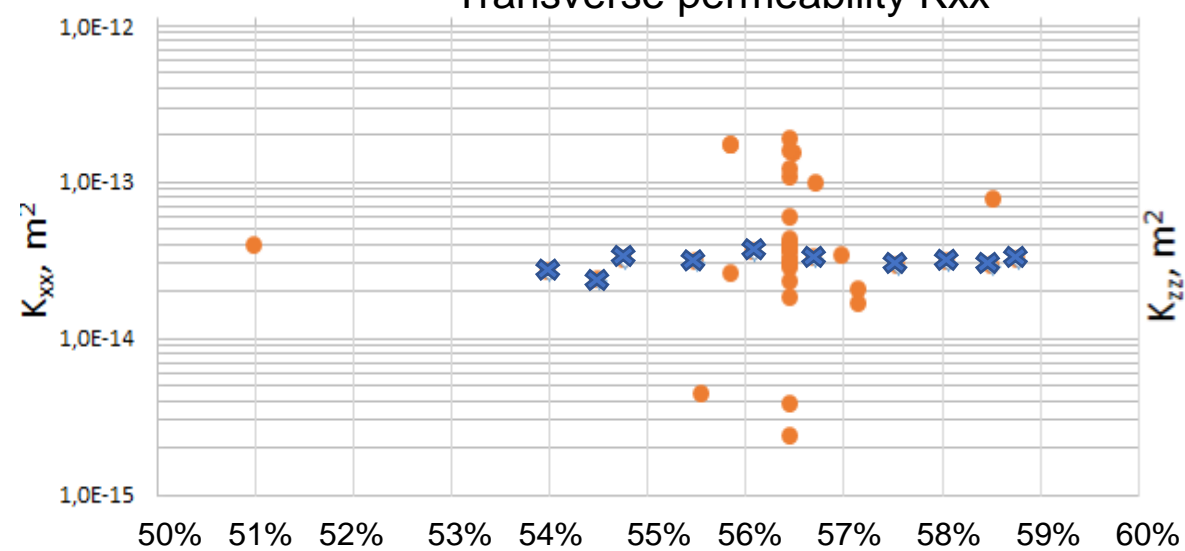
➤ Cluster of values at FVC = 56.46% has a CV of 16%.

Correlation with fiber volume content

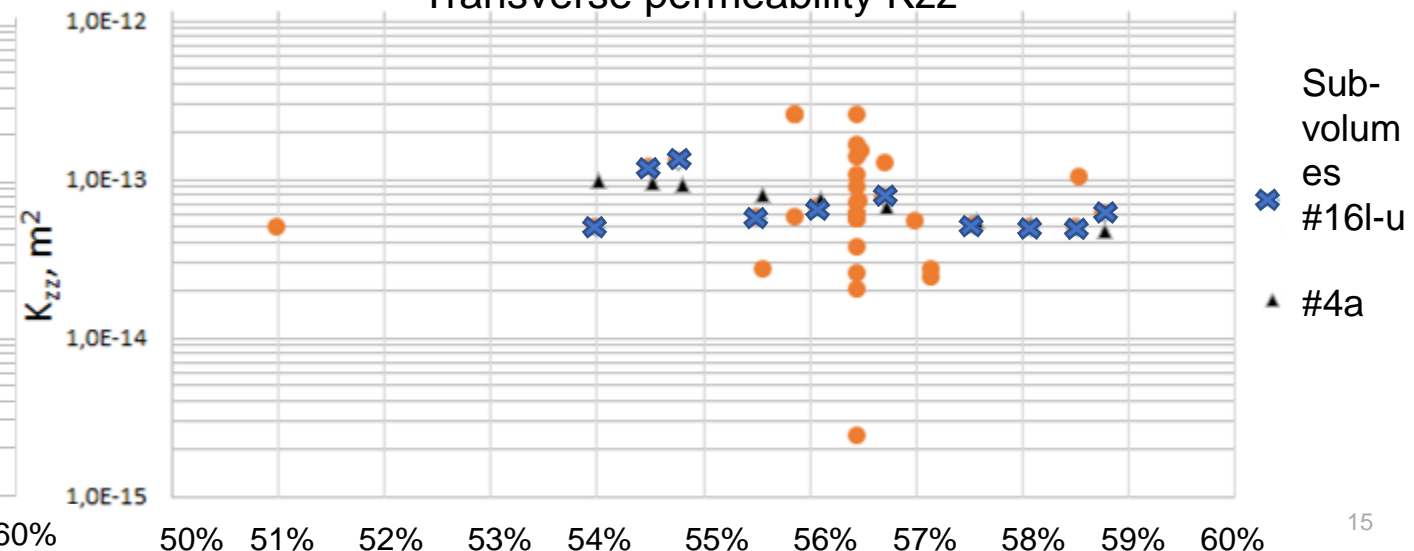
Axial permeability K_{yy}



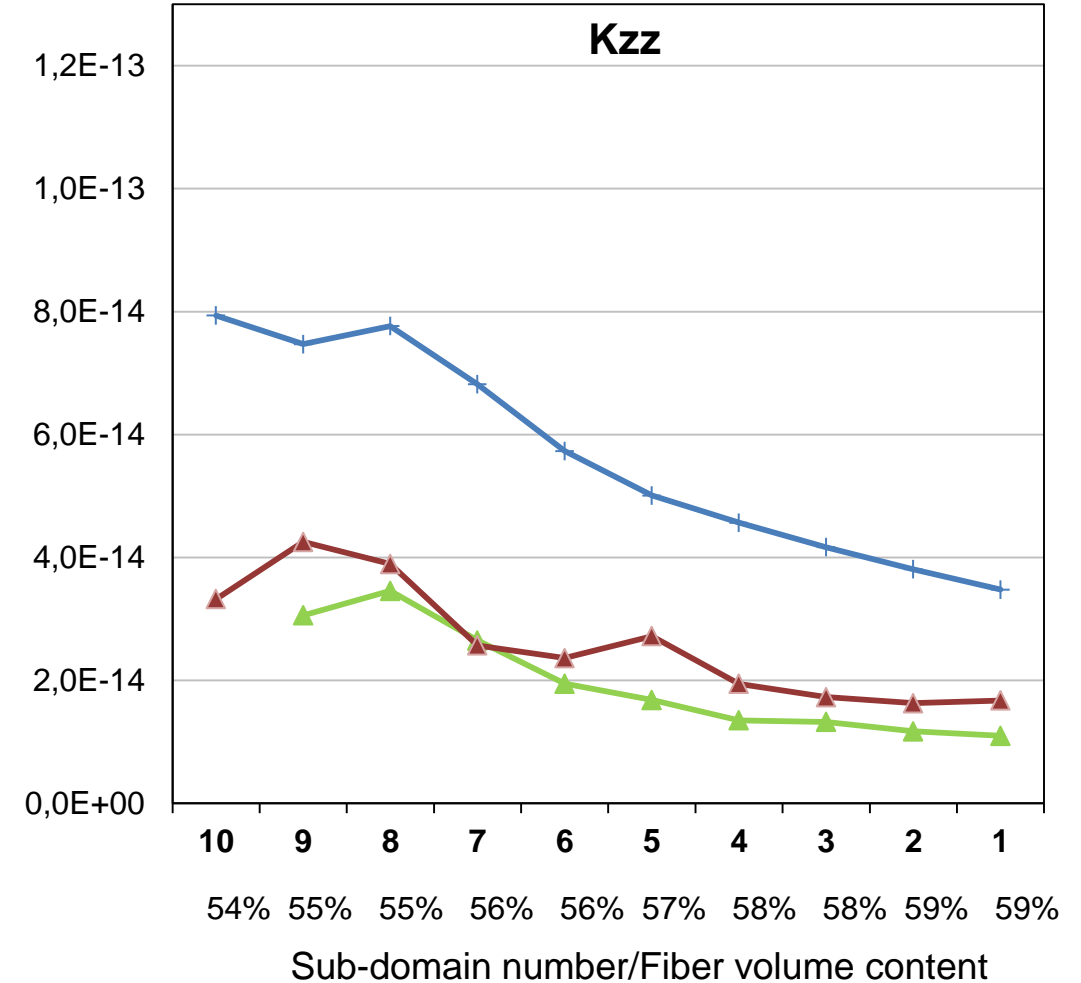
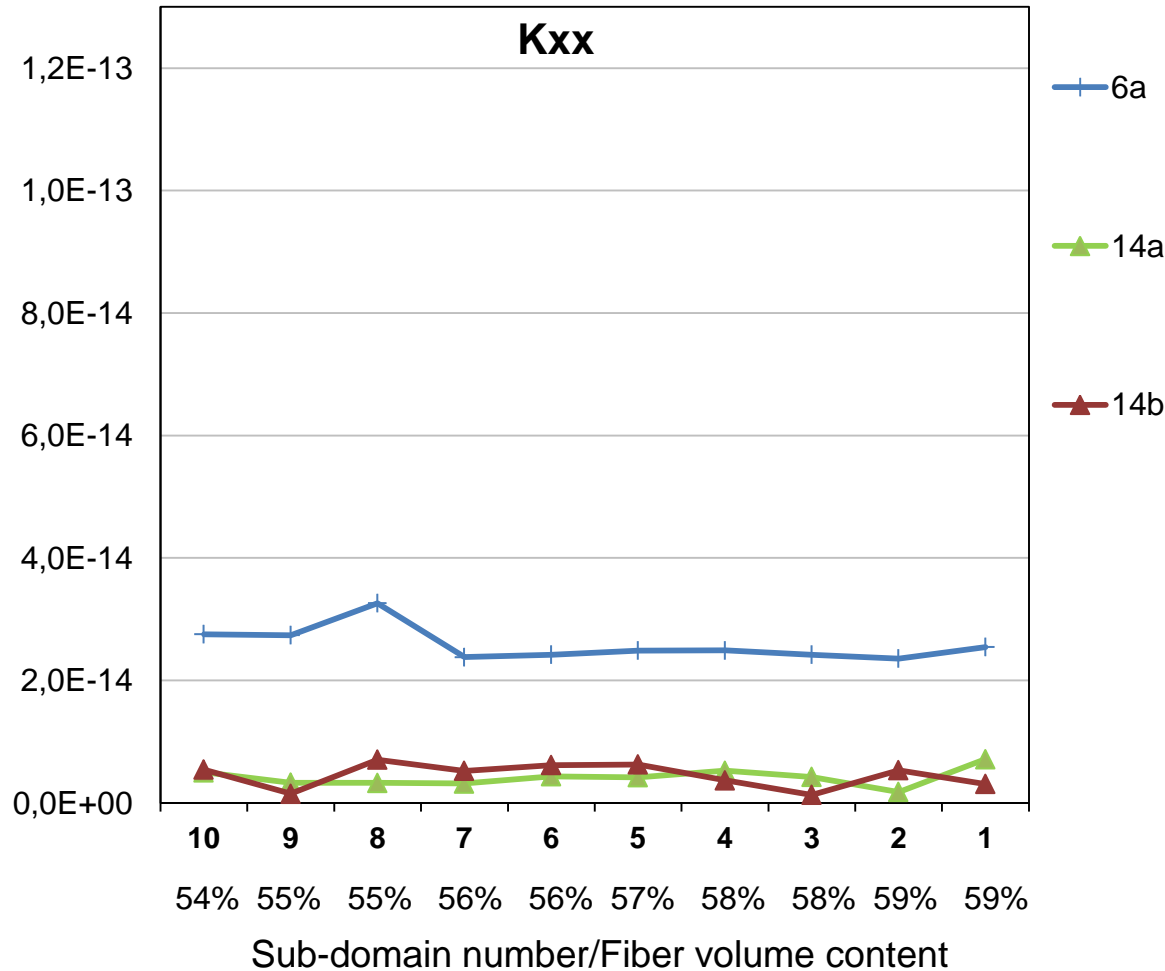
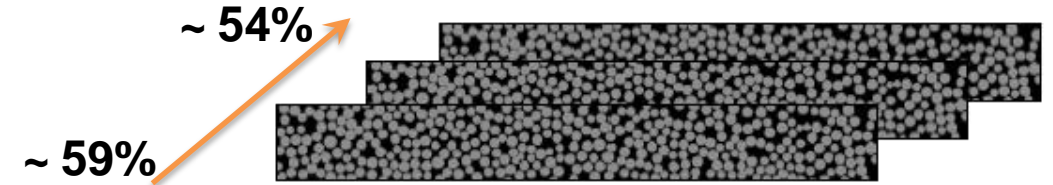
Transverse permeability K_{xx}



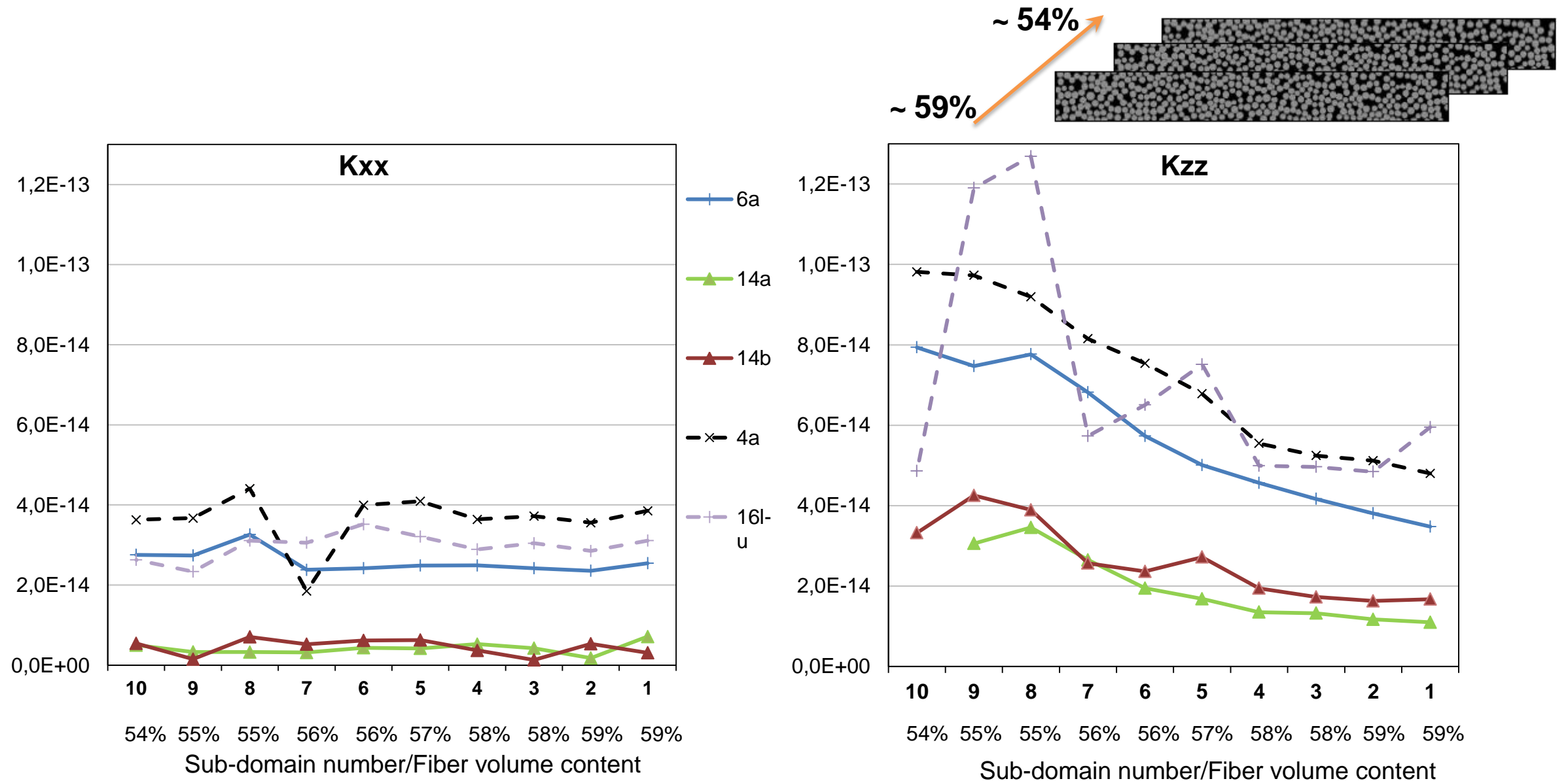
Transverse permeability K_{zz}



Correlation with fiber volume content: 2D/3D

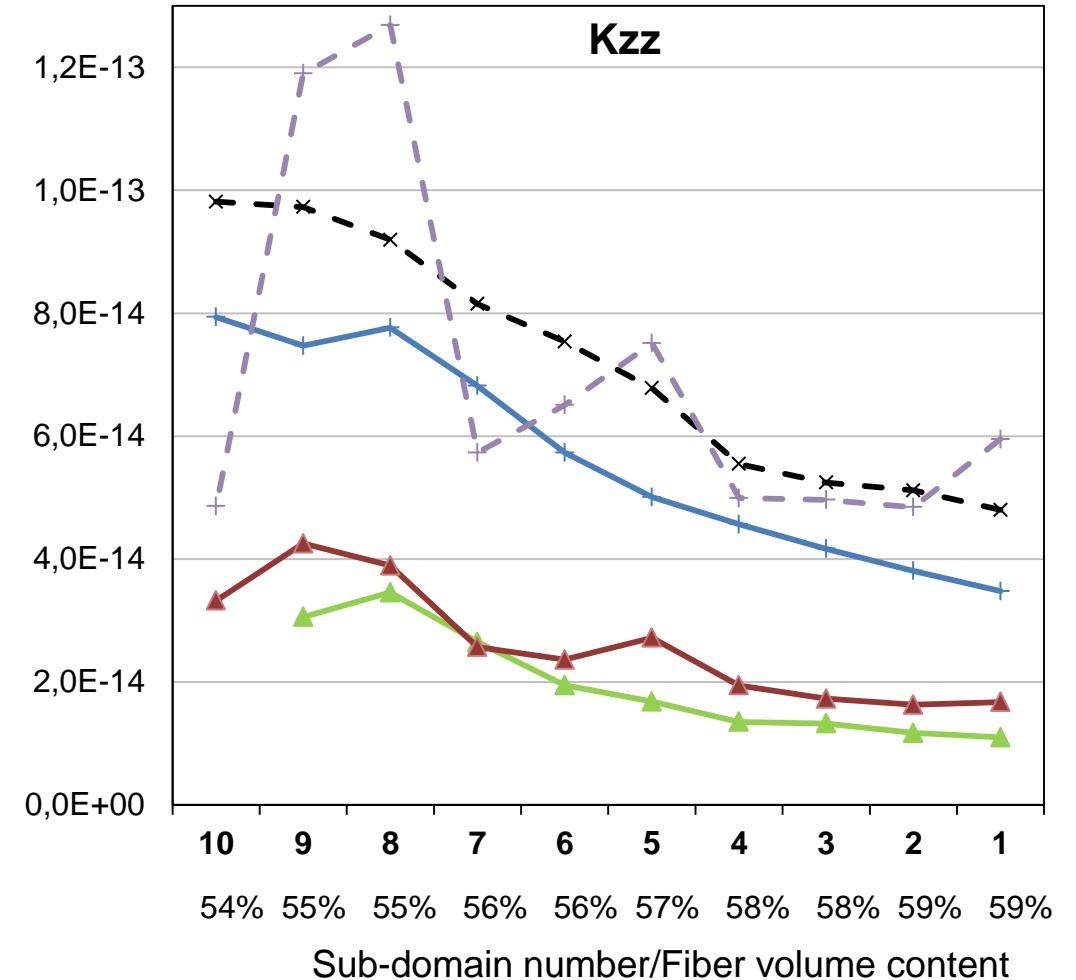
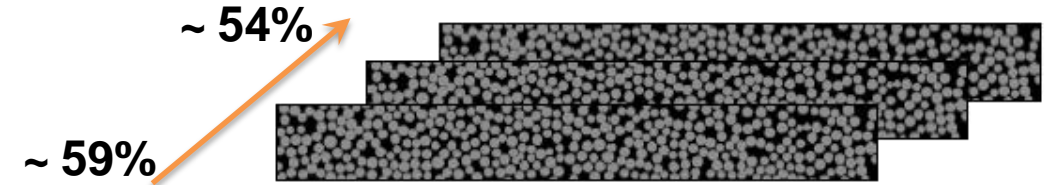
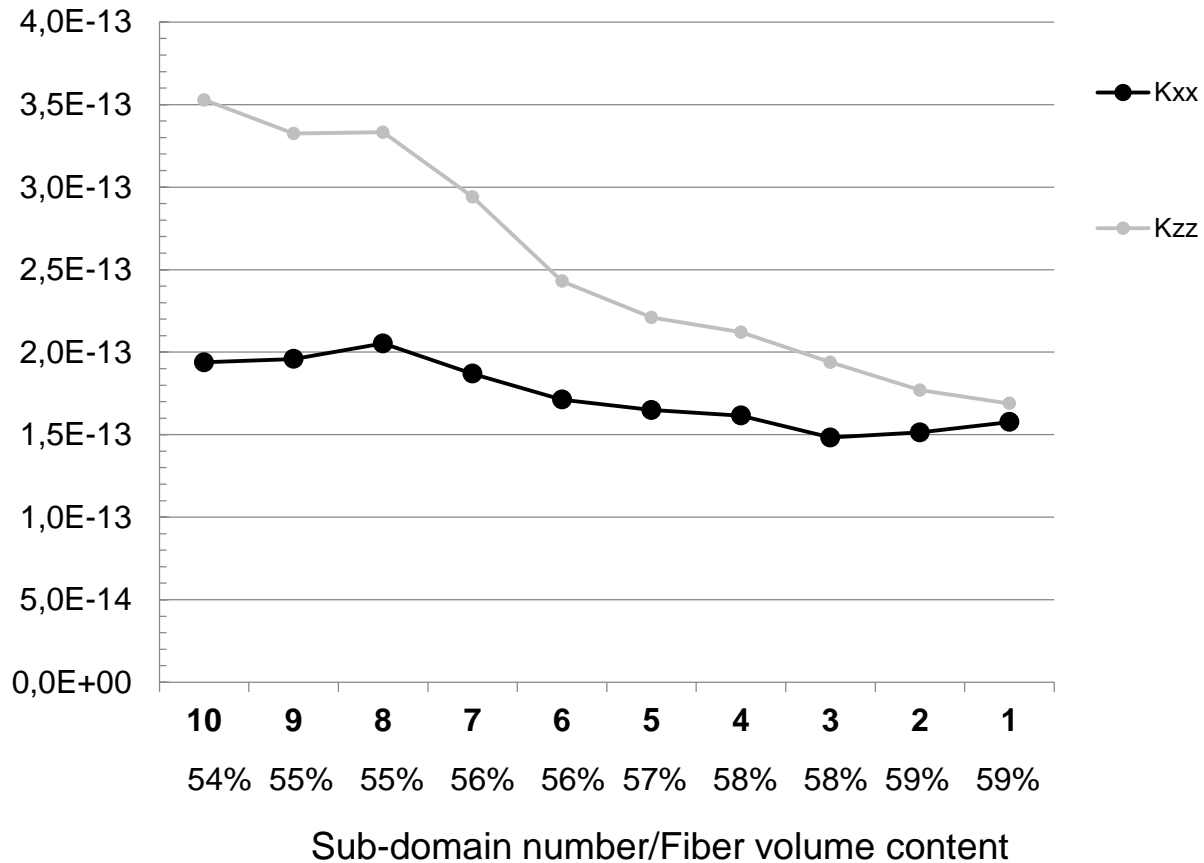


Correlation with fiber volume content: 2D/3D

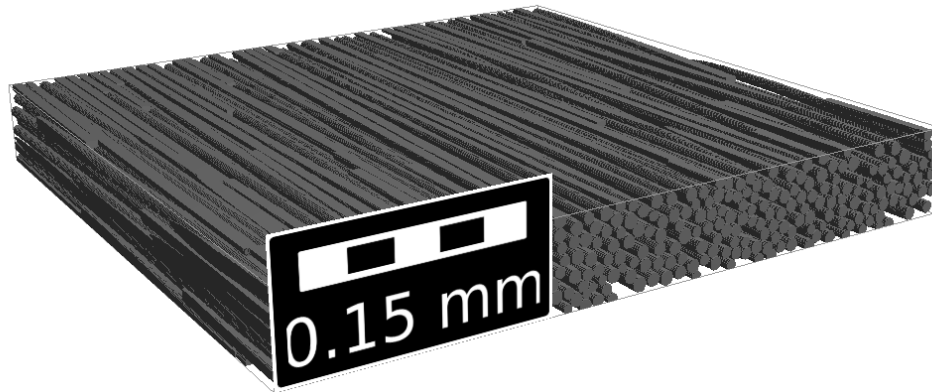


Correlation with fiber volume content: 2D/3D

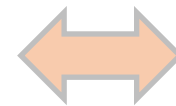
Transverse components of result #6b,c:
identification with Darcy's law **accounting for the cross-flows**



Real sample

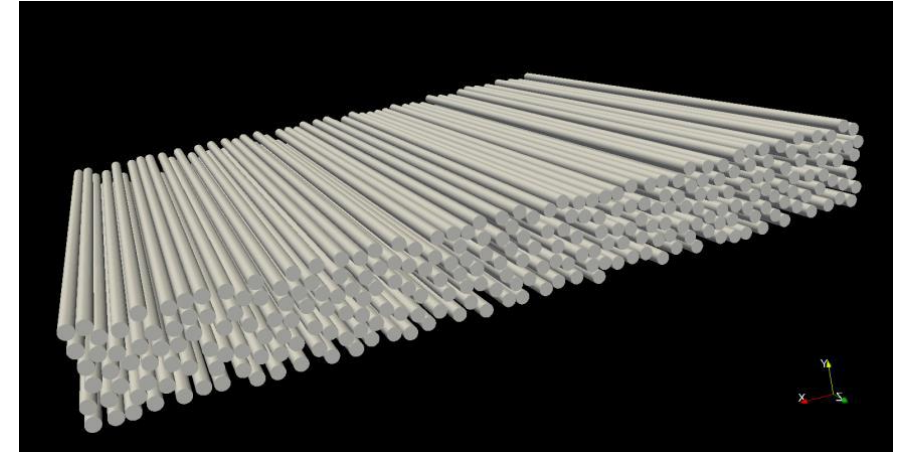


- Varying FVC 54-59% along the fibre direction
- Varying fibre diameter 7.5-9.3 μm



Digital twin

(generated by random sequential addition method in #15b)



- Constant FVC 51% along the fibre direction
- Constant fibre diameter 9 μm

Assumptions:

- fibres perfectly aligned
- constant fibre diameter
- no twist

	K_{xx}, m^2	K_{yy}, m^2	K_{zz}, m^2
CV	69%	40%	69%

Correlation between results #15a (image) and #15b (digital twin) using the same method

❑ After detailed analysis of results => reduced coefficient of variation

❑ Importance of calculation of full permeability tensor, which is a symmetric positive definite second order tensor. Stokes equation to address the creeping flow condition.

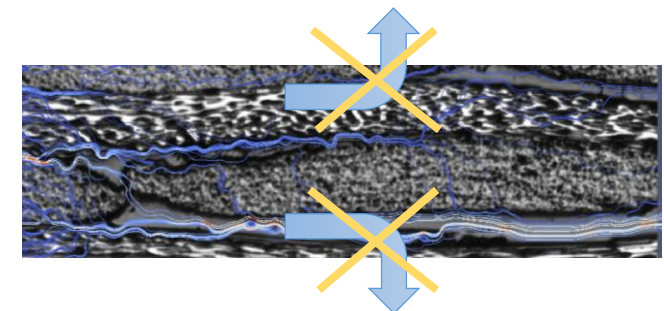
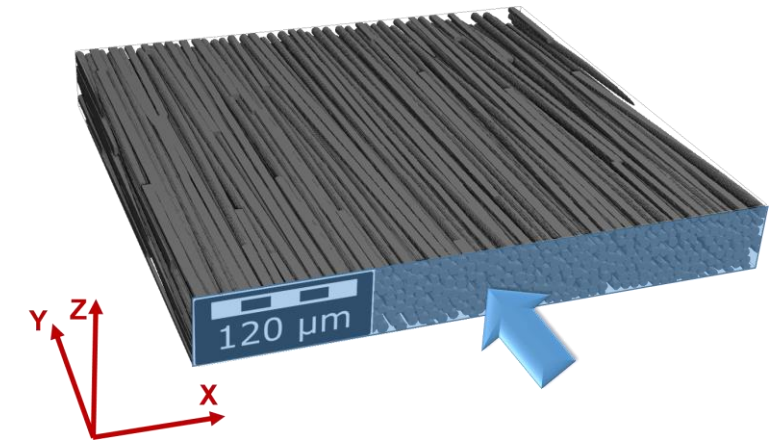
❑ Dominant effect of:

- permeability identification technique;
- BC in tangential direction (compared to the BC in flow direction);
- number of sub-domains used in renormalization technique.

❑ When principal directions of flow are unknown, no-slip and symmetric BC are not convenient.

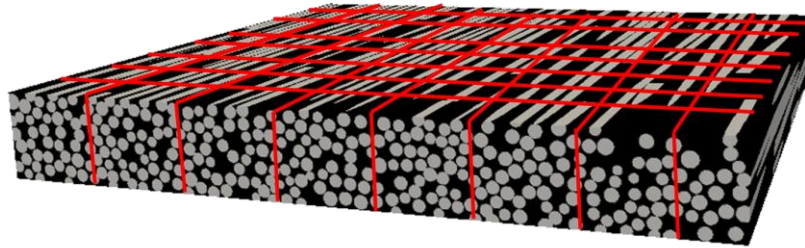
Resulting cluster of permeability values

	K_{xx}, m^2	K_{yy}, m^2	K_{zz}, m^2
Mean	3.2E-14	9.4E-13	5.2E-14
CV	24%	14%	25%



Summary and conclusions

- ❑ Subdivision into sub-domains with subsequent renormalization can be a reasonable solution, but highly dependent on:
 - i) number of sub-domains;
 - ii) presence of transverse anisotropy effects in the microstructure.



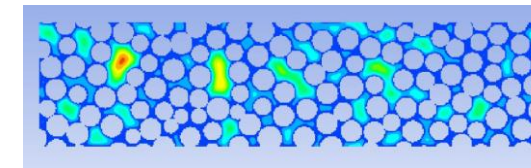
- ❑ No definite conclusion on the correlation of 2D/3D solutions based on the results of the benchmark for this type of microstructure.

➡ To access 3D image data of the first stage of the benchmark on the repository:

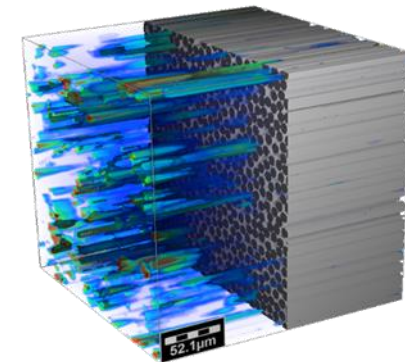
<https://doi.org/10.5281/zenodo.6611926>

Resulting cluster of permeability values

	K_{xx}, m^2	K_{yy}, m^2	K_{zz}, m^2
Mean	3.2E-14	9.4E-13	5.2E-14
CV	24%	14%	25%

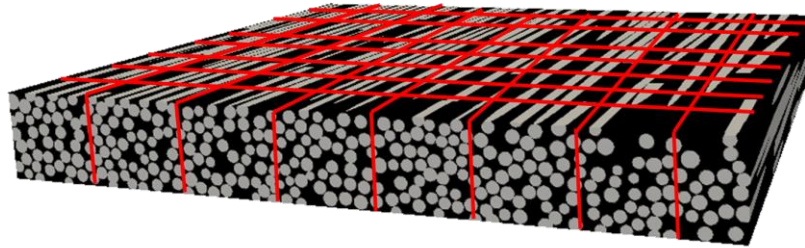


From reporting #3



Summary and conclusions

- ❑ Subdivision into sub-domains with subsequent renormalization can be a reasonable solution, but highly dependent on:
 - i) number of sub-domains;
 - ii) presence of transverse anisotropy effects in the microstructure.

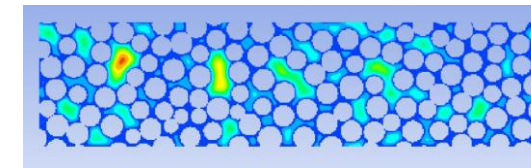


- ❑ No definite conclusion on the correlation of 2D/3D solutions based on the results of the benchmark for this type of microstructure.

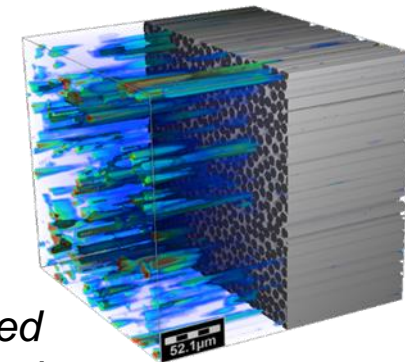
- *E. Syerko, T. Schmidt, D. May, C. Binetruy, S.G. Advani et al. Benchmark Exercise on Image-Based Permeability Determination of Engineering Textiles: Microscale Predictions // Composites Part A: Applied Science and Manufacturing 2022 (submitted).*

Resulting cluster of permeability values

	K_{xx}, m^2	K_{yy}, m^2	K_{zz}, m^2
Mean	3.2E-14	9.4E-13	5.2E-14
CV	24%	14%	25%

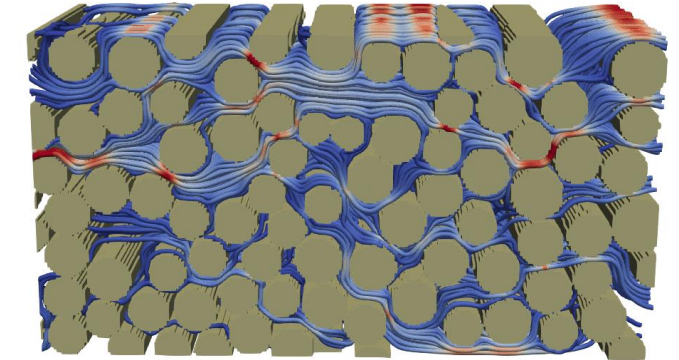
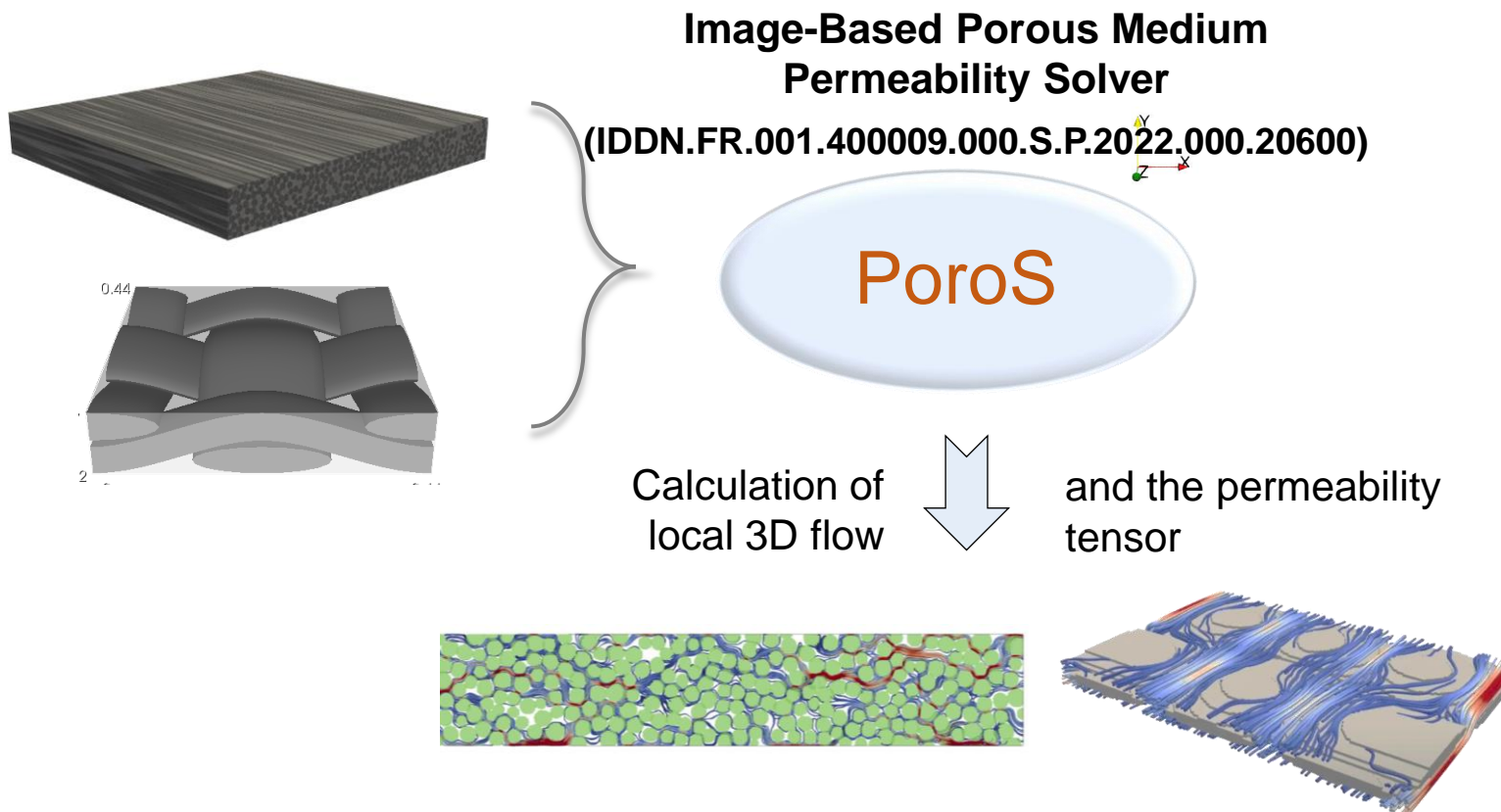


From reporting #3



In-house developed solution PoroS

- Stokes / Brinkman solver;
- Pseudo-compressibility formulation;
- Homogenization technique for permeability tensor calculation based on the equivalence of dissipated at different scales powers.



Flow calculated through the fibrous
structure sample

- Values situated within the cluster of benchmark results.

- **Second stage of the Virtual Permeability Benchmark** at meso-scale of the material is on-going until December 31st 2022.



For further questions on the Virtual Permeability Benchmark you can contact:



Dr. Elena Syerko

@ elena.syerko@ec-nantes.fr

☎ +33 2 40 37 16 96



Tim Schmidt

@ tim.schmidt@ivw.uni-kl.de

☎ +49 631 2017 469